Exergy analysis of a cooling system: experimental investigation on the consequences of the retrofit of R22 with R422D

Ciro Aprea[1], Angelo Maiorino[1*] and Rita Mastrullo[2]

[1]Department of Industrial Engineering, University of Salerno, Via Ponte Don Melillo 1, 84084 Fisciano, SA, Italy; [2]DETEC, University of Naples Federico II, P.le Tecchio 80, 80125 Napoli, NA, Italy

Abstract

In this article, the performances of a walk-in air cooler working with R22 and its substitute R422D are experimentally studied. To define a full comparison on the performance characteristics of R22 and R422D, both an energetic and an exergetic analyses are proposed. The experimental investigation was carried out considering four levels of refrigeration capacity: 920, 1340, 1925 and 2250 W. All tests were run at steady-state conditions and by keeping the value of the external air temperature equal to 22°C. The experimental analysis allowed the determination of the COP, the exergetic efficiency, the exergy flow destroyed in each component and other variables characterizing the working of the plant. The results demonstrated that COP of R422D is, on average, 20% lower than that of R22. Furthermore, for plant whose condenser is air cooled, R422D could lead to increase the fan speed or to adopt bigger blowers.

Keywords: exergy; experimentation; R22; refrigerant; retrofitting; R422D

*Corresponding author:
amaiorino@unisa.it

Received 21 May 2012; revised 28 June 2012; accepted 19 July 2012

1 INTRODUCTION

R22 has been widely used as refrigerant in air conditioning and in medium and low-temperature applications within the commercial and industrial refrigeration. Owing to its ozone-depleting effect, Montreal Protocol and its amendments have set the phase-out deadlines on R22 in different countries and areas. European Union and Japan have banned the import of R22 systems since 2004, and the USA will prohibit the use of R22 as refrigerant in new equipment from 2010 and so on. In accordance with Montreal Protocol, China, as developing country, will freeze R22 consumption at its level in 2015, and will ban the use of R22 in A/C industry from 2040 and so on. With increasingly understanding the consequences caused by the ozone depletion, many countries and areas have accelerated the phase-out process of R22.

During the last few years, new trends in the use of refrigerants have been established depending on the application field as highlighted in Cavallini *et al.* [1], Billiard [2] and UNEP [3]. The substitution of R22 is an operation that will interest many plants, which are expected still working after its phase-out. The drop-in candidates for R22 have been checked for environmental and safety requirements, compatibility with lubricant oil, filters and sealing. Among the candidates, to establish the best substitute in a specified system, it is necessary to estimate energetic performances after substitution. In the last few years, many companies have expended much effort to develop and identify the refrigerants able to increase the energetic efficiency of a refrigerating system, depending on its application. In the same way, many researchers have investigated on the energetic performances of the newest substitutes of R22. Stegou-Sagia [4] carried out the irreversibility analysis in a single-stage vapor-compression cycle with refrigerant mixtures R404A, R410A, R410B and R507. Aprea *et al.* [5] performed the exergetic analysis of a vapor compressor refrigeration plant for R22 and its substitutes R407C, R417A and R507C. In their experiments, varying the speed of the compressor motor controlled

International Journal of Low-Carbon Technologies 2014, 9, 71–79

doi:10.1093/ijlct/cts060 Advance Access Publication 27 August 2012

the refrigeration capacity. Their results established that R407C is the most suitable substitute of R22 in variable speed applications. Another way was considered by Lorentzen and Pettersen [6], which proposed a return to the use of carbon dioxide as refrigerant, in order to reduce drastically the direct environmental impact. Many authors have carried out various experimental works in order to test the energetic performances of carbon dioxide refrigeration systems [7–9]. However, when working under transcritical conditions, carbon dioxide systems have extremely high working pressure, low operation efficiency and high operation and capital costs.

During this transition period, many industrial and commercial applications have used R407C to retrofit R22. Even if R407C has thermophysical properties similar to those of R22 and it is nonflammable and nontoxic, it has the disadvantage of not being suitable with mineral or alkylbenzene oils. Furthermore, in comparison with R22, experimental tests carried out with R407C have pointed out a reduction in the energetic performances with a lager environmental impact [10].

Recent additions to the aforementioned alternative refrigerants for R22 are R422A, R422B, R422C and R422D. The US environment protection agency reported that these alternative refrigerants could be used for household and light-commercial air-conditioning applications. In our precedent work [11], we have demonstrated that, for an R22 refrigeration system retrofitted with R422D, the TEWI could increase up to 36.8%. Furthermore, we have shown this increase was due both to the higher GWP of R422D and to the decrease of the energy performances consequently to retrofit with R422D. In the same time, we identified some operating scenarios for which the retrofit with R422D reduce the TEWI; in particular, some eco-friendly scenarios result technically feasible and it can be obtained by both reducing the leakage rate of refrigerant and increasing the overall efficiency of the plant. While the reduction of the leakages of refrigerant is well known like technical solution, the increase of the overall efficiency for refrigeration systems retrofitted with R422D is worthy of investigation. In fact, the result of a bibliographic research showed that, until now, few works have been published on this argument. Arora and Sachdev [12] performed a theoretical energetic and exergetic analysis of R422 series. They found that, for R422 series refrigerants, the throttle valve and the compressor are the worst components from the viewpoint of efficiency defects. In addition, they showed that R422 series refrigerants could cause a deterioration of COP. Torrella *et al.* [13] presented an experimental comparative study of the operation of a water chiller with the refrigerant R22 and the R422D. They observed a decrease both of the cooling capacity and of the power consumption with regard to the operation with R22 when the chiller worked with the R422D; consequently, they demonstrated that a small improvement of the energy performances is obtainable with the substitution of the R22 with R422D.

The aim of this article is to show how to improve the overall efficiency of the refrigeration plants retrofitted with R422D; for this purpose, we propose an experimental investigation, and an exergetic analysis able to point out what components cause the decrease of the performances of a refrigeration plant retrofitted with R422D. In particular, our experimental study is referred to a commercial walk-in air cooler operating at four different operating conditions in terms of refrigeration capacity.

2 COMPARISON ON THE PROPERTIES OF R22 AND R422D

R422D is an easy-to-use, non-ozone-depleting HFC refrigerant originally designed to replace R22 in existing direct expansion water chiller systems. It can also be used in residential and commercial air conditioning and medium- to low-temperature refrigeration systems. As suggest by DuPont [14], minor equipment modifications (replacing of the filter drier and elastomeric seals/gaskets that are exposed to refrigerant, refill of oil if required) or expansion device adjustments may be required in some applications. Although, in general, the same seal materials can be used with R422D, it has been observed that shrinkage of the original seal may occur after conversion causing refrigerant leakage; in particular, it is preferable to substitute the seals of the valve plate in the compressor, of the liquid level receiver gaskets, of the solenoid valves and of the flanges.

Furthermore, compressor manufactures specify that there are no mechanical side effects in using R422D.

Table 1 shows the specific composition and relevant data of R22 and R422D. Figure 1 shows that the vapor pressure curves for the two fluids are very similar, while a slight difference occurs between the liquid pressure curves.

In the temperature range of −40 to 40°C and pressure of 100–1800 kPa, it is possible to draw the following observations between the refrigerants in terms of thermodynamic properties. The heat of vaporization is ∼20% higher for R22 than that for R422D (Figure 2). The liquid densities are approximately the same for R22 and R422D, while the vapor density is higher for R422D than that for R22. Both the liquid heat capacity and the vapor heat capacity are 15–25% higher for R422D, and the difference increases with the increase of the pressure. The liquid and the vapor viscosities are approximately the same for R22

Table 1. *Refrigerants data.*

	R22	R422D
Composition (% wt)	$CHClF_2$	31.5% R134a 65.1% R125 3.4% R600a
ODP	0.05	0
GWP (100 years)	1700	2230
Bubble point temperature, 100 kPa (°C)	−40.8	Z43.5
Critical temperature (°C)	96.1	79.6
Saturated vapor pressure at 40°C (kPa)	1533.6	1555.0
Glide temperature at 40°C vapor saturation pressure (°C)	0	2.46
Glide temperature at 0°C vapor saturation pressure (°C)	0	3.56

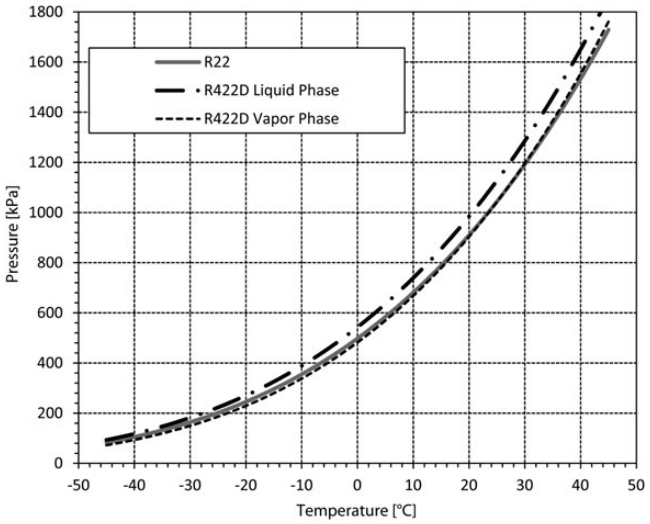

Figure 1. *Graphical comparison of saturation pressure vs. temperature of R422D and R22.*

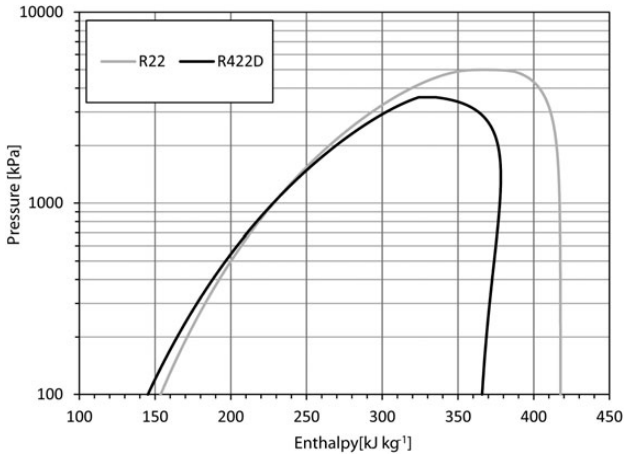

Figure 2. *Pressure–enthalpy diagram for refrigerant R22 and R422D.*

and R422D. The liquid conductivity is around 18% higher for R22, and the vapor conductivity is 25% higher for R422D [15].

R422D is a mixture of refrigerants (Table 1) and, as a nonazeotropic, has the ability to fractionation, thus each refrigerant boils at different temperature in the vapor stage. This causes the temperature of a nonazeotropic to greatly increase as it passes through the evaporator and greatly decrease in the condenser. However, the temperature glide difference of the R422D results less than that of R407C.

3 EXPERIMENTAL TESTS

An experimental investigation was carried out to compare the energetic and exergetic performance characteristics of R22 and R422D. Experiments were performed on a vapor compression refrigeration plant for a walk-in cooler.

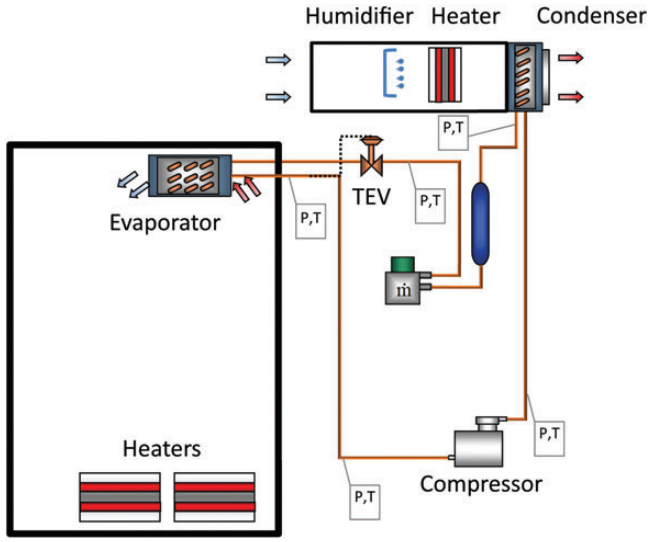

Figure 3. *Sketch of the experimental plant.*

Table 2. *Compressor specifications.*

Characteristics of the compressor	
Typology	Semihermetic
Power supply	400 V 50 Hz
Displacement	3.86 $m^3 h^{-1}$
Number of cylinders	2
MOP	22 bar (LP) 30.5 bar (HP)
Oil type	mineral 32 cSt
Refrigerating capacity (R134a working fluid)	At 35°C condensing temperature −15 to +20°C evaporating temperature 730–4360 W

As declared by the manufacturer.

3.1 Experimental facility

The experimental vapor compression refrigeration plant, applied to a commercially available walk-in cooler as shown in Figure 3, consists of a semihermetic reciprocating compressor (Table 2), an air condenser followed by a liquid receiver, an R22 thermostatic expansion valve to feed an air-cooled evaporator inside the walk-in cooler. As declared by the manufacturer of the walk-in cooler, the thermal conductance of the wall is equal to 0.208 $Wm^{-2} K^{-1}$; consequently, we estimated the leakage of heat through the wall is limited to 120 W, when the difference between the inner temperature and that outer is equal to 30 K.

The compressor, as declared by the manufacturer, can work with R22 and mineral oil.

During the retrofit operations, the factory setting of the R22 thermostatic expansion valve was changed in order to keep the operating superheat conditions for R422D in the same range

used for R22. This was obtained by tuning the valve adjustment screw.

A blower drove the airflow through a thermally insulated channel, where some electrical resistances were installed with the objective of controlling the temperature of the airflow across the condenser. In order to control the temperature of the airflow, a PID controller energized the electrical resistances, while a humidifier kept the right wet-bulb temperature. Additional electrical heaters wired to a voltage regulator simulated the cooling load in the cold reservoir. To keep the air temperature reasonably constant in the cold reservoir, an on/off refrigeration control system was implemented. Turning on/off the compressor and the fan of the heat exchangers does this.

Table 3 reports the specifications of the transducers used (Coriolis effect mass flow rate meter, RTD 100 4 wires calibrated thermoresistances, piezoelectric absolute pressure gauge, wattmeter and humidity sensor). The thermoresistances were located outside the pipe, with a layer of heat transfer compound (aluminum oxide plus silicon) placed between the sensor and the pipe to provide good thermal contact. The whole pipe was covered with 25-mm thick flexible insulation. The system of temperature measurement was checked against a sensor positioned in pocket in a similarly insulated pipework. For various test conditions, the difference between the two measurements has been always $<0.3^{\circ}$C.

The test apparatus is equipped with 32-bit A/D converter acquisition cards linked to a personal computer. A software application, called FrigoCheck v.1.0., has been developed by the authors. The software is able to evaluate in real time the COP, the entropy and the enthalpy of all points of the thermodynamic cycle; furthermore, it shows the whole cycle on P-h diagram and it establishes when the system is the steady state.

3.2 Experimental procedure

Air heaters and humidifiers guaranteed the operating conditions at condenser. During all tests the relative humidity in the inner cooler was below 50%. The refrigeration load was supplied by an electrical heaters placed in the walk-in cooler; in addition, additional load was caused by the heat exchanges with outdoor through the wall of the walk-in cooler. All tests were run at steady-state conditions and by keeping the value of the superheat in a narrow range: 7.0–10.0°C. Temperature and pressure values in key points of the plant were continuously monitored, to evaluate when the system was operating under steady-state conditions.

Table 3. *Transducers specifications.*

Transducers	Range	Uncertainty
Coriolis effect flowmeter	0–2 kg min^{-1}	±0.2%
RTD 100 4 wires	−100 to 500°C	±0.15°C
Piezoelectric absolute pressure gauge	1–10 bar	±0.2%
	1–30 bar	±0.5% F.S.
Wattmeter	0–3 kW	±0.2%

With the purpose of testing the behavior of the plant under different load conditions, we identified four levels of the refrigeration load in accordance with typical operating conditions of a walk-in cooler used as food storage and processing.

The tests have been performed at four levels of refrigeration capacity: 920, 1340, 1925 and 2250 W. All tests were run at steady-state conditions while the air temperature at the condenser was equal to 24°C, and the relative humidity was included in the range 50–60%. Data were recorded after the plant operated under steady-state conditions for 1 h at the specified test conditions. The plant approached the steady-state operation when:

- the temperatures of saturated refrigerant corresponding to the measured refrigerant-side pressures had maximum variations of ±1.7°C of the average values;
- the fluctuations of the refrigerant mass flow rates were within 2% of the readings.

4 ENERGETIC AND EXERGETIC ANALYSIS

The overall energetic performance of the plant has been defined by evaluating its coefficient of performance, calculated as the ratio between the refrigeration capacity and the electrical power supplied to the plant (compressor, fans and accessories):

$$\mathrm{COP} = \frac{\dot{m}(h_{\mathrm{out,EV}} - h_{\mathrm{in,EV}})}{\dot{W}_{\mathrm{el}}} \tag{1}$$

where COP is the coefficient of performance, and the term at numerator correspond to the cooling capacity defined as the heat absorbed by the refrigerant at the evaporator, $\dot{m}$ is the mass flow rate (kg s^{-1}), $h_{\mathrm{in,EV}}$ and $h_{\mathrm{out,EV}}$ are the enthalpies of input and output of the evaporator, respectively (kJ kg^{-1}). $\dot{W}_{\mathrm{el}}$ is the electrical power supplied to the plant (W).

The exergetic analysis reveals important information about the plant total irreversibility distribution among the components, determining which component weighs more on the overall plant inefficiency. In accordance with Kotas [16], we have calculated the exergy flow destroyed in each component of the refrigeration plant by means of the following equations:

$$\dot{\mathrm{E}}\mathrm{x}_{\mathrm{des,EV}} = \dot{m}(h_{\mathrm{in,EV}} - T_0 s_{\mathrm{in,EV}}) + \dot{Q}_{\mathrm{EV}}\left(1 - \frac{T_0}{T_{\mathrm{r}}}\right) - \dot{m}(h_{\mathrm{out,EV}} - T_0 s_{\mathrm{out,EV}}) \tag{2}$$

$$\dot{\mathrm{E}}\mathrm{x}_{\mathrm{des,CP}} = \dot{m} T_0 (s_{\mathrm{out,CP}} - s_{\mathrm{in,CP}}) \tag{3}$$

$$\dot{\mathrm{E}}\mathrm{x}_{\mathrm{des,CO}} = \dot{m}(h_{\mathrm{in,CO}} - T_0 s_{\mathrm{in,CO}}) - \dot{m}(h_{\mathrm{out,CO}} - T_0 s_{\mathrm{out,CO}}) \tag{4}$$

$$\dot{\mathrm{E}}\mathrm{x}_{\mathrm{des,VA}} = \dot{m} T_0 (s_{\mathrm{out,VA}} - s_{\mathrm{in,VA}}). \tag{5}$$

where $\dot{\mathrm{E}}\mathrm{x}_{\mathrm{des,EV}}$, $\dot{\mathrm{E}}\mathrm{x}_{\mathrm{des,CO}}$, $\dot{\mathrm{E}}\mathrm{x}_{\mathrm{des,VA}}$ are the exergy rates of fluid destroyed in the evaporator, condenser and expansion valve, respectively (kW). T_0 and T_{r} are the temperatures at the dead

state 0 and in the space to be cooled, respectively (K). $\dot{Q}_{EV}$ is the thermal power of the evaporator (W). $s_{in,EV}$ and $s_{out,EV}$ are the entropies of input and output of the evaporator, respectively (kJ kg^{-1} K^{-1}). $s_{in,CP}$ and $s_{out,CP}$ are the entropies of input and output of the compressor, respectively (kJ kg^{-1} K^{-1}). $h_{in,CO}$ and $h_{out,CO}$ are the enthalpies of the input and output of the condenser, respectively (kJ kg^{-1}). $s_{in,CO}$ and $s_{out,CO}$ are the entropies of input and output of the condenser, respectively (kJ kg^{-1} K^{-1}). $s_{in,VA}$ and $s_{out,VA}$ are the entropies of input and output of the expansion valve, respectively (kJ kg^{-1} K^{-1}).

In addition, the overall plant exergetic efficiency has been evaluated as:

$$\eta_{ex} = 1 - \frac{\sum_i \dot{E}x_i}{\dot{m}(h_{out,CP} - h_{in,CP})} \quad (6)$$

where η_{ex} is the exergetic efficiency, $h_{in,CP}$ and $h_{out,CP}$ are the enthalpies of the input and output of the compressor, respectively (kJ kg^{-1}).

5 ERROR ANALYSIS

In accordance with the procedure suggested by Moffat [17], Fatouh and Elgendy [18] and Sun [19], we developed an error analysis for the quantity indirectly evaluated as the compression ratio, the COP, the exergy flow destroyed and the exergetic efficiency.

The overall error S is associated to a quantity indirectly evaluated G from the measured values of the variables X_i:

$$S = \pm\sqrt{\sum_{i=1}^{n} S^2(X_i)}. \quad (7)$$

In order to solve Equation (7), we have to know the expression of the function, which links the quantity G to its variables X_i. When this expression is unknown, like in the case of the enthalpy and the entropy, we can referee to the procedure suggested by Moffat [18]. Therefore, considering Equations (1 to 6) in addition with the uncertainties presented in Table 3, we obtained that the overall error of the quantity indirectly evaluated were those reported in Table 4.

Table 4. *Uncertainty for the quantity indirectly evaluated.*

Quantity G	Uncertainty (%)
COP	2.1–3.2
$\dot{E}x_{des,EV}$	1.1–1.9
$\dot{E}x_{des,CP}$	1.5–2.1
$\dot{E}x_{des,CO}$	1.3–1.7
$\dot{E}x_{des,VA}$	2.2–3.0
η_{ex}	2.5–4.2

6 RESULTS AND DISCUSSIONS

For each level of the refrigeration capacity, the temperature of the air contained in the cold store is reported in Figure 4. The temperature curves of R22 and R422D are nearly overlapping each other. Figure 5 shows the variation of COP with the refrigeration capacity both for R22 and for R422D. It is possible to observe that COP increases with the increase of the refrigeration capacity and that the COP for R22 is higher than for R422D. In particular, the difference between the COP for R22 and for R422D is, on average, 20% and it decreases with the increase of the refrigeration capacity. Arora and Sachdev [12] proposed a similar result, and they underlined that this is disadvantageous in terms of overall environmental pollution, because more fuel must be burned and higher amounts of carbon dioxide are discharged in the atmosphere. When R422D is used as refrigerant, the reduction of energy performances in terms of COP is due to the increase of the electrical power absorbed. As the blowers and the other accessories used

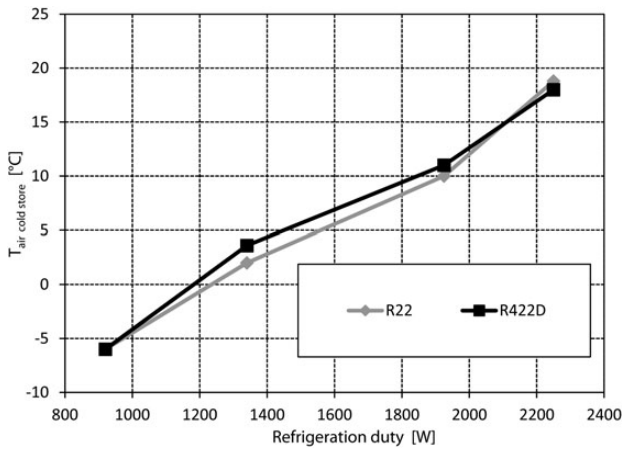

Figure 4. *Comparison of cold store temperature vs. refrigeration duty for R22 and R422D.*

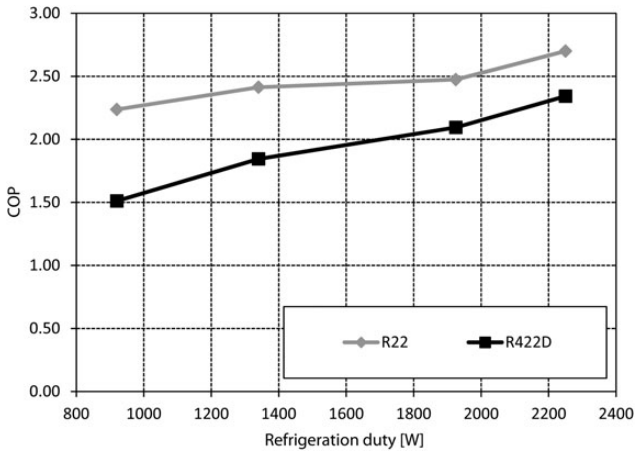

Figure 5. *Comparison of COP vs. refrigeration duty for R22 and R422D.*

in all tests were the same, the gain of electrical power absorbed was due to the augmentation of the compression power. As reported in Table 5, the specific work of compression is, on average, 10% higher for R22 than for R422D, because the vapor density of R422D is higher than that of R22 (Section 2). Jointly, the mass flow rate of R422D results higher than that of R22 (Figure 6). As aforementioned, the heat of vaporization is higher for R22 than that for R422D, and then a higher mass flow rate of R422D is required to even the cooling load: during our tests, the mass flow rate of R422D has been 45% higher than that of R22. Considering that the compression ratio has been slightly higher for R422D than for R22 (Figure 7), it is possible to state that the retrofit with R422D leads to a higher mass flow rate of refrigerant mainly because the density of R422D at suction is higher than that of R22 (Table 6). Looking at Equation (1) and considering that electrical power absorbed by the compressor is directly proportional to the mass flow rate, it is understandable that COP does not depend on the mass flow rate. Consequently, it is possible to state that when R422D is used as a substitute of R22 and the same cooling power is provided, the COP of the plant decreases due both to the high gain of the specific work of compression and to the loss of the heat of vaporization.

During the tests, the working of the compressor was regular and no technical problem occurred. It is important to report that during the operating of the plant with R422D the level of oil in the compressor did not decreased. It is well known that the presence of R600a in the mixture makes easy the return of the oil, which leaves the compressor. The temperature of R422D at compressor outlet was, on average, 20°C lower than that of R22 (Figure 8). The reduction of the temperature at

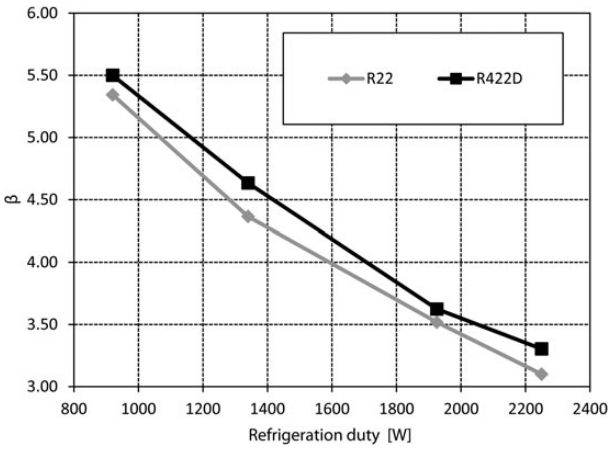

Figure 7. *Comparison of compression ratio vs. refrigeration duty for R22 and R422D (uncertainty equal to 0.85%).*

Table 5. *Specific work of compression values for R22 and R422D.*

Refrigeration duty (W)	$w^{a}_{CP,R22}$(kJ kg^{-1})	$w^{a}_{CP,R422D}$ (kJ kg^{-1})
920	61.4	57.9
1340	51.7	45.3
1925	48.0	39.4
2250	40.2	37.6

w is the specific work of compression.
[a]Uncertainty equal to ± 0.4 (kJ kg^{-1}).

Table 6. *Density values for R22 and R422D.*

Refrigeration duty (W)	ρ^{a}_{R22} (kg m^{-3})	ρ^{a}_{R422D} (kg m^{-3})
920	9.54	13.90
1340	15.57	19.57
1925	19.23	27.04
2250	22.98	28.94

ρ is the density of the refrigerant.
[a]Uncertainty equal to ± 0.61 (kg m^{-3}).

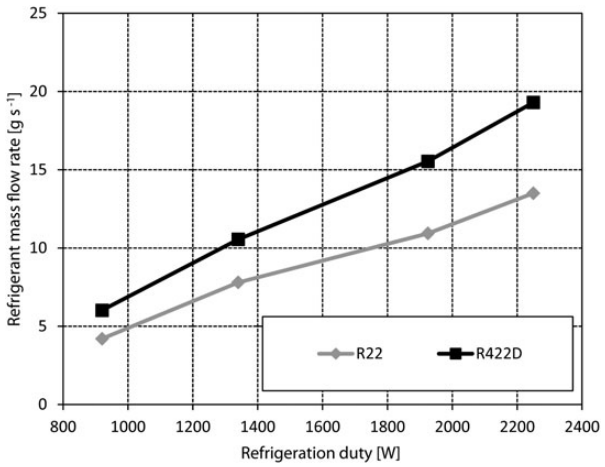

Figure 6. *Comparison of mass flow rate vs. refrigeration duty for R22 and R422D.*

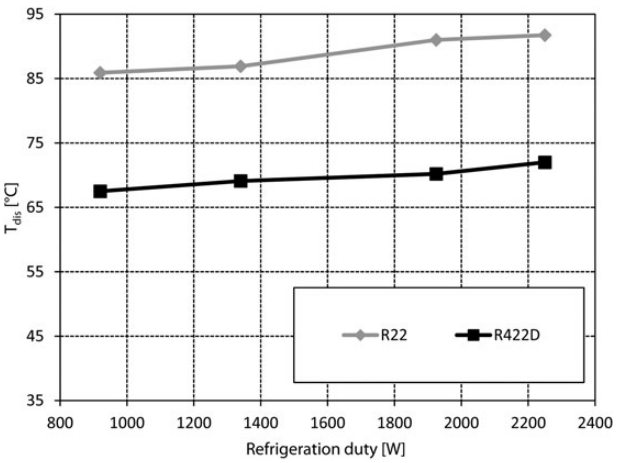

Figure 8. *Comparison of discharge temperature vs. refrigeration duty for R22 and R422D.*

compressor outlet is a benefit, in fact, as suggested by Arora and Sachdev [12], this could lead to a longer life of the compressor with R422D in comparison with R22. As reported in Figure 9, the pressure of R422D at compressor outlet was higher than that of R22. The gain of the discharge pressure was not the cause of risk for the life of the compressor: the maximum increment of the pressure was equal to 15%, which was less than the maximum working pressure declared by the manufacturer of the compressor.

The increase of condensing pressure shows that, when R422D is used as refrigerant, the heat exchange surface of the condenser is not enough to reject the thermal power. Even if the discharge temperature of R422D is lower than that of R22, it is important to observe that the temperature of R422D at outlet of the condenser is higher than that of R22 (Figure 10). This circumstance occurred because the thermal power rejected at condenser was higher for R422D than for R22 (Table 7), while the heat exchange surface and the fan speed were the same for both refrigerants.

As aforementioned, the experimental plant adopts a thermostatic expansion valve as expansion device. For each test condition, both for R22 and for R422D the operating superheat was included in a narrow range of 7.0–10.0°C.

In Figure 11, the change of the evaporation temperature with the refrigeration capacity is reported both for R22 and for R422D (in the case of the mixture, it means the initial temperature of evaporation). It is possible to observe that the temperature curves of R22 and R422D increase with the increase of the refrigeration capacity; furthermore, the temperature curves of both refrigerants are nearly overlapping each other. For all test conditions, the glide temperature difference of R422D during the evaporation phase was, on average, equal to 6°C [15]. Then, it is noticeable that both refrigerants have a similar behavior at evaporator; this is explainable if one

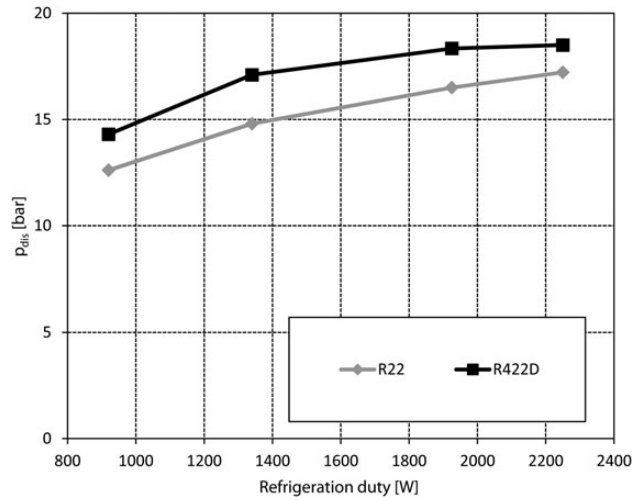

Figure 9. *Comparison of discharge pressure vs. refrigeration duty for R22 and R422D.*

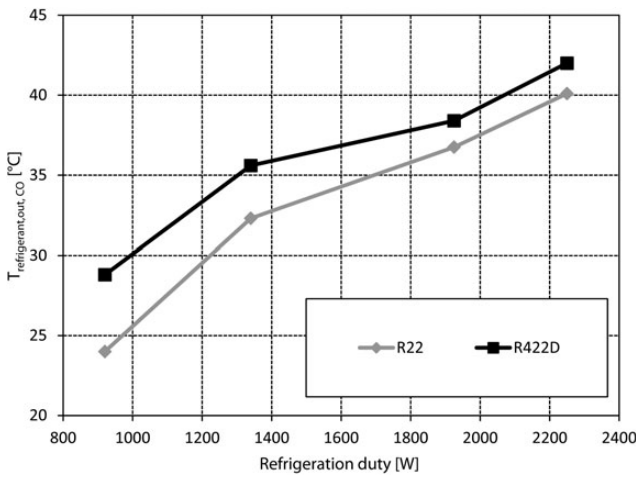

Figure 10. *Comparison of temperature at outlet of condenser vs. refrigeration duty for R22 and R422D.*

Table 7. *Thermal power rejected at condenser and subcooling at condenser outlet values.*

Refrigeration duty (W)	Q^{a}_{rej} (W)		Δ^{b}_{sc} (°C)	
	R22	R422D	R22	R422D
920	1026	1050	7.5	5.8
1340	1298	1654	6.2	5.7
1925	1801	2320	6.5	5.8
2250	2792	2990	6.4	5.8

[a]Uncertainty equal to ±4 (W).
[b]Uncertainty equal to ±0.2 (°C).

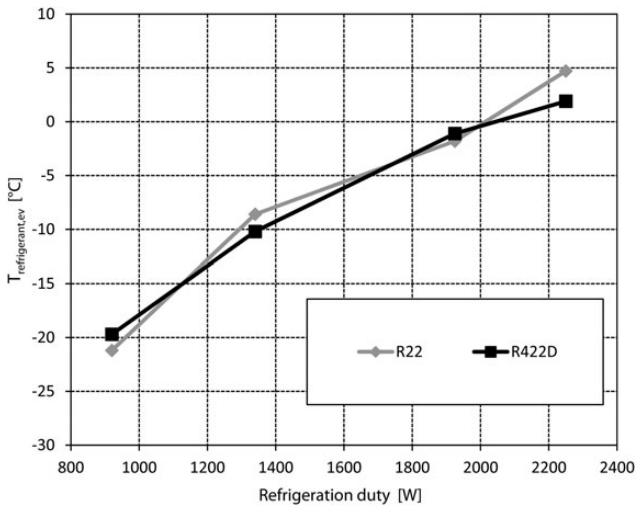

Figure 11. *Comparison of evaporation temperature vs. refrigeration duty for R22 and R422D (in the case of the mixture it means the initial temperature of evaporation).*

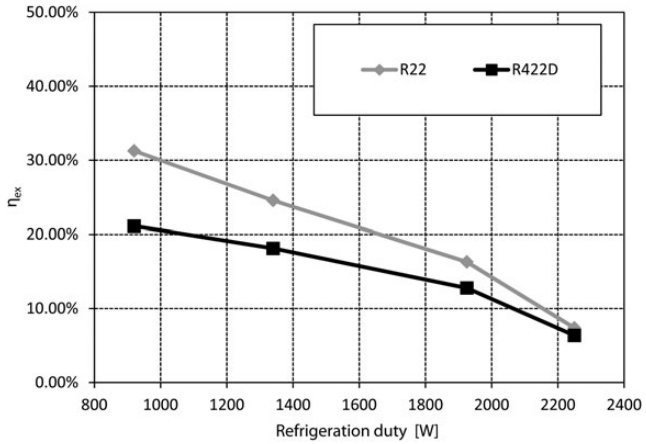

Figure 12. *Comparison of exergetic efficiency vs. refrigeration duty for R22 and R422D.*

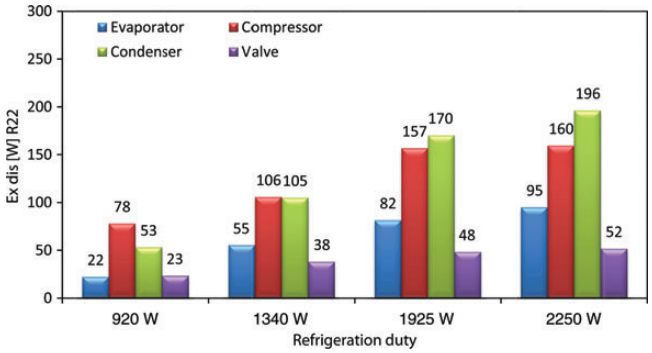

Figure 13. *Distribution of the exergy flow destroyed by each component vs. refrigeration duty for R22.*

considers that the difference between the heat transfer coefficient of R422D and that of R22 has no influence for an air evaporator, because the heat transfer coefficient of the air is much lower than those of both refrigerants are. As both the thermal power and the heat exchange surface were the same and, furthermore, the glide temperature difference of R422D was very low, the results shown in Figures 4 and 11 are justified.

Figure 12 shows the variation of the exergetic efficiency with the refrigeration capacity both for R22 and for R422D. It is possible to observe that the exergetic efficiency decreases with the increase of the refrigeration capacity and that the exergetic efficiency for R22 is higher than for R422D. In particular, the difference between the exergetic efficiency for R22 and for R422D decreases with the increase of the refrigeration capacity: it ranges between 21 and 6%. This result can lead to state that R22 produces more product exergy for less input exergy in comparison with R422D. In order to investigate on the reduction of exergy efficiency due to the retrofit of R22 made with R422D, in Figures 13 and 14, the values of the exergy flow

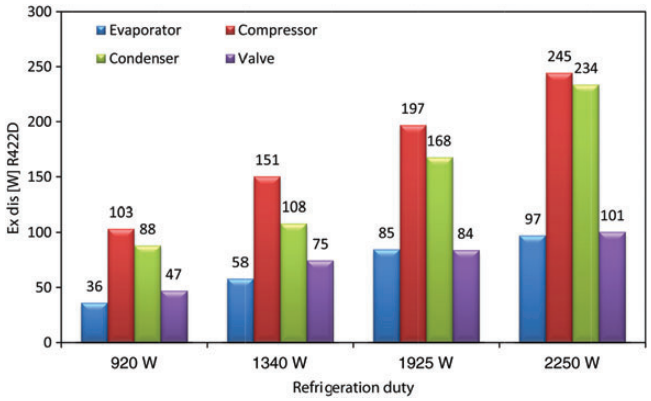

Figure 14. *Distribution of the exergy flow destroyed by each component vs. refrigeration duty for R422D.*

destroyed in each component of the plant are reported for both refrigerants. Comparing the Figures 13 and 14, it is possible to observe:

- The retrofit of R22 made with R422D causes a gain of exergy flow destroyed for each component and for each test condition. This circumstance is mainly connected to the higher mass flow rate of R422D than that of R22.
- When R22 is used as refrigerant, the condenser is the largest cause of the exergy flow destroyed.
- When R422D is used as refrigerant, the compressor and the condenser are both the largest cause of the exergy flow destroyed. In particular, under the point of view of the exergy flow destroyed, the compressor results the worst component of the retrofitted plant.
- Owing to the adoption of R422D, the compressor increases its exergy flow destroyed by 40%, because the discharge pressure of R422D is higher than that of R22.
- By working with R422D, the valve greatly increases its exergy flow destroyed by 95%, both because of the higher discharge pressure of R422D and because of the higher temperature of the refrigerant at outlet of the condenser.
- The exergy flow destroyed at the evaporator is higher for R422D than for R22. This circumstance is mainly due to the higher mass flow rate of R422D than that of R22. Anyway, this difference looks less to that expected because of the slight fluctuations of refrigeration power that occurred between the two refrigerants for each test condition.

7 CONCLUSIONS

An experimental investigation was carried out to compare the energetic and exergetic performance characteristics of R22 and R422D. Experiments were carried out by means of a vapor compression refrigeration plant applied to a cold store. For both refrigerants four levels of refrigeration capacity were

investigated: 920, 1340, 1925 and 2250 W. All tests were run at steady-state conditions and keeping the value of the superheat in a narrow range: 7.0–10.0°C. Based upon the experimental results, the following conclusions were drawn.

(1) The experimental results demonstrated that COP of R422D is, on average, 20% lower than that of R22. It has been showed that, when R422D is used as refrigerant, the reduction of energy performances in terms of COP is due to the increase of the electrical power absorbed because of the higher mass flow rate of R422D required to even the cooling load.
(2) During the tests, the mass flow rate of R422D has been 45% higher than that R22. This huge gain of mass flow rate is obtainable since the density of R422D at suction is higher than that of R22.
(3) R422D showed a discharge pressure 15% higher than that of R22, but no technical problem occurred, because the levels of pressure were less than the maximum working pressure of the compressor.
(4) R422D showed a discharge temperature 20°C lower than that of R22, and then it is possible to state that R422D offers longer compressor life.
(5) The change of the evaporation temperature with the refrigeration capacity is approximately the same for both refrigerants; furthermore, R422D showed a low glide temperature difference during the evaporation phase: 6°C.
(6) Exergetic efficiency of R22 is better than that of R422D. In particular, the difference between the exergetic efficiency for R22 and for R422D decreases with the increase of the refrigeration capacity: it ranges between 21 and 6%.
(7) The retrofit of R22 made with R422D leads to an increment of exergy flow destroyed for each component. This circumstance is mainly connected to the higher mass flow rate of R422D than that of R22.
(8) The largest increasing of exergy flow destroyed due to retrofit of R22 with R422D occurs at valve and at compressor. In particular, the exergy flow destroyed at valve increases by 95%, while at compressor it increases by 40%.

REFERENCES

[1] Cavallini A. Working fluids for mechanical refrigeration. *Int. J. Ref.* 1996;**19**:485–96.
[2] Billiard F. New trends in refrigerating equipment and refrigerants. In: *Proceedings of 10th European Conference on Technological Innovations in Air Conditioning and Refrigeration Industry*, Milan, Italy, 2003.
[3] Report of the refrigeration, air-conditioning and heat pumps technical options committee. United Nations Environment Programme. 2006.
[4] Stegou-Sagia A. Evaluation of mixture efficiency in refrigerating system. *Energy Convers Manage* 2005;**46**:2787–802.
[5] Aprea C, de Rossi F, Greco A et al. Refrigeration plant exergetic analysis varying the compressor capacity. *Int J Environ Res* 2003;**27**:653–69.
[6] Lorentzen G, Pettersen J. New possibilities for non-CFC refrigeration. In Pettersen J (ed). *International Institute of Refrigeration International Symposium on Refrigeration, Energy and Environment*. 1992, 147–63.
[7] Cavallini A, Cecchinato L, Corradi M et al. Two-stage transcritical carbon dioxide cycle optimisation: a theoretical and experimental analysis. *Int J Refrig* 2005;**28**:1274–83.
[8] Cabello R, Sànchez D, Llopis R et al. Experimental evaluation of the energy efficiency of a CO2 refrigerating plant working in transcritical conditions. *Appl Therm Eng* 2008;**28**:1596–604.
[9] Aprea C, Maiorino A. Heat rejection pressure optimization for a carbon dioxide split system: An experimental study. *Appl Energy* 2009;**86**:2373–80.
[10] Aprea C, Mastrullo R, Renno C et al. An evaluation of R22 substitutes performances regulating continuously the compressor refrigeration capacity. *Appl Therm Eng* 2004;**24**:127–39.
[11] Aprea C, Maiorino A. An experimental investigation of the global environmental impact of the R22 retrofit with R422D. *Energy* 2011;**36**:1161–70.
[12] Arora A, Sachdev HL. Thermodynamics analysis of R422 series refrigerants as alternative refrigerants to HCFC22 in a vapor compression refrigeration system. *Int J Environ Res* 2009;**33**:753–65.
[13] Torrella ER,, Cabello D, Sánchez JA et al. Llopis. On-site study of HCFC-22 substitution for HFC non-azeotropic blends (R417A, R422D) on a water chiller of a centralized HVAC system. *Energy Build* 2010;**42**:1561–66.
[14] Retrofit guidelines for DuPont™ Isceon® M029 (R422D) Refrigerant, Du Pont Techincal Information ART.46. http://www.refrigerants.dupont.com, 2007.
[15] Lemmon EW, McLinden MO, Huber ML. *NIST Reference Fluid Thermodynamic and Transport Properties Database (REFPROP), Version 7.0*, National Institute of Standards and Technology, 2002.
[16] Kotas TJ. *The Exergy Method of Thermal Plant Analysis*. Krieger Pub. Co., ISBN: 9780894649462, 1995.
[17] Moffat RJ. Using uncertainty analysis in the planning of an experiment. *TransASME, J Fluids Eng* 1985;**107**:173–8.
[18] Fatouh M, Elgendy E. Experimental investigation of a vapor compression heat pump used for cooling and heating applications. *Energy.* 2011;**36**:2788–95.
[19] Sun G. Experimental investigation of integrated refrigeration system (IRS) with gas engine, compression chiller and absorption chiller. *Energy.* 2008;**33**:431–6.